

## A study of the electrochemical properties of lead–strontium alloys for lead/acid batteries

**Wen Haiquan\*** and **Sheng Fenchi**

*Nanjing Storage Battery Plant, 32 Heilongjiang Rd., Nanjing 210037, Jiangsu (China)*

**Su Wenduan** and **Zhou Shaomin**

*Department of Chemistry, Xiamen University, Xiamen (China)*

### Abstract

The electrochemical properties of lead–strontium alloys have been investigated by using a dynamic potential technique and scanning electron microscopy (SEM). The results show that the alloys appear more resistant to corrosion than traditional lead–antimony alloys or modern lead–calcium alloys. Perhaps, there is relatively perfect phase-structure in the lead-oxide layer on the alloy surface that is responsible for this corrosion-resistant behaviour.

### Introduction

Antimony has been used as grid material in lead/acid batteries for over 100 years. But the disadvantages of antimony in terms of self-discharge with increasing rate, and evolution of gas (including toxic stibine) during over-charging [1] are well established. Various antimony-free alloys have been studied. At present, only the lead–calcium system is used in both the cast and the wrought forms as grids of maintenance-free automotive, telephone standby and small portable batteries. Nevertheless, calcium-bearing alloys have often demonstrated poor processing characteristics and, in particular, some problems in deep-cycling lead/acid batteries.

Positive-grid corrosion is a critical problem with the lead/acid battery. In order to increase the anti-corrosion of grids, considerable efforts have been made [2] in the search for additives to improve the electrochemical properties of both Pb–Sb and Pb–Ca alloys. Nevertheless, it has not been possible to increase the anti-corrosion of Pb–Sb or to solve the problem related to the great amount of gas evolution during charging. Besides, the use of Pb–Ca alloys is limited due to its difficulty in casting, narrow range of tolerance, and sensitivity to deep discharge.

Recently, a new lead–strontium alloy, used in grids of the 3XM10 sealed battery, has been manufactured by the Nanjing Storage Battery Plant. Performance testing of the 3XM10 design has shown that the Pb–Sr battery is promising for deep-cycling applications and for long-life services.

---

\*Author to whom correspondence should be addressed.

This paper reports of a study of the corrosion current versus time curves for Pb-Sb alloys in the temperature range 18 to 50 °C, and at potentials 0 to 1.45 V (versus  $\text{Hg}/\text{Hg}_2\text{SO}_4/5.3 \text{ M H}_2\text{SO}_4$ ). Polarization curves and cyclic voltammograms were investigated before and after corrosion. The corrosion films were observed by means of scanning electron microscopy (SEM). Finally, the electrochemical properties of these alloys were compared with those of antimony and calcium alloys under the same experimental conditions.

## Experimental

Four lead alloys consisting of  $\text{X}_1$  (Pb-0.07wt.%Sr),  $\text{X}_2$  (Pb-0.07wt.%Sr-0.02wt.%Xt, Xt denotes Ce mischmetal), B (Pb-4.18wt.%Sb) and A (Pb-0.11wt.%Ca) were cast into cylinder (electrode I: diameter 5 mm; height 20 mm; electrode II: diameter 5 mm; height 40 mm) and rectangular (electrode III:  $25 \times 10 \times 3$  mm) electrodes, respectively. The composition of these alloys was determined using the ICP technique. Electrode I was fixed in a glass tube with epoxy and its exposed part was cut to give an inclined plane of 45° with a surface area of approximately 0.14 cm<sup>2</sup>. This electrode was used for polarization curves and cyclic voltammetric studies. Electrode II was located in a glass tube with epoxy; it had a working surface of approximately 10.56 cm<sup>2</sup> and was used for corrosion testing. Electrode III was polished and corroded at constant potential; its surface was then observed under SEM.

The electrolyte used in all experiments was 5.3 M  $\text{H}_2\text{SO}_4$  prepared from A.R. grade sulphuric acid and doubly-distilled water. The temperature was controlled to  $\pm 1^\circ\text{C}$  by a water bath. The potential was held constant to  $\pm 1$  mV with a three-electrode potentiostat. The reference electrode was  $\text{Hg}/\text{Hg}_2\text{SO}_4/5.3 \text{ M H}_2\text{SO}_4$ ; all potentials are reported with respect to this electrode. The counter electrode was made from platinum. The working current was monitored as a function of time or potential by a microcomputer system.

## Results

Each electrode III was polished and cleaned, then placed in 5.3 M  $\text{H}_2\text{SO}_4$  and corroded for 4 h at 50 °C under a constant potential of +1.45 V. After formation of the corrosion films, the electrodes were rinsed with distilled water and dried with filter paper. The corrosion films were examined by SEM (Fig. 1). As can be seen from Fig.1, a net-like corrosion layer exists on the Pb-Sb alloy surface. This may be due to intergranular corrosion of the antimony-rich phase. By contrast, the corrosion layer on the other alloy samples has a more uniformly distributed morphology.

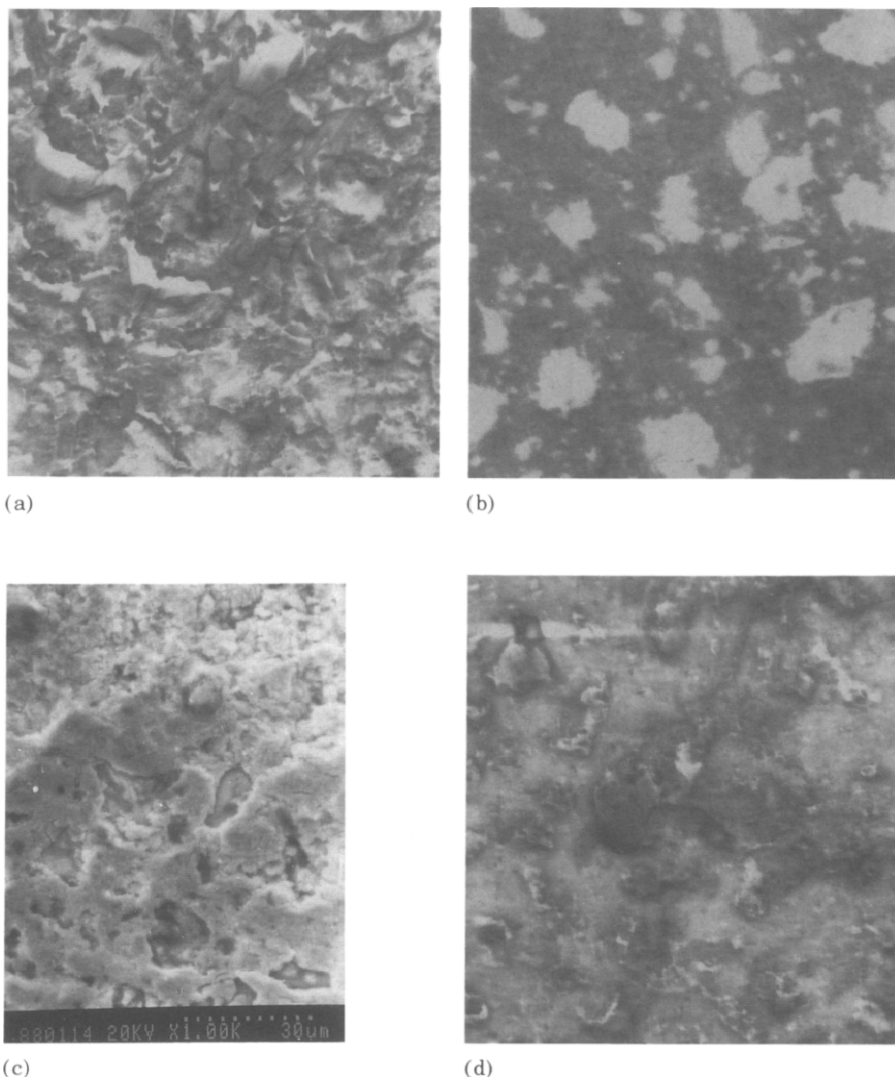


Fig. 1. Electron micrographs of alloy electrodes after corrosion. (a) electrode A, Pb-0.11wt.%Ca; (b) electrode B, Pb-4.18wt.%Sb; (c) electrode X<sub>1</sub>, Pb-0.07wt.%Sr; (d) electrode X<sub>2</sub>, Pb-0.07wt.%Sr-0.02wt.%Xt.

Each electrode II was treated in 20% NaOH + 15% sucrose solution at 80 °C for 2 min, then was taken out and rinsed with distilled water, and placed in 5.3 M H<sub>2</sub>SO<sub>4</sub> to corrode at +1.45 V for 8 h at 50 °C. The relationship between corrosion current and time is shown in Fig. 2. It was found that oxygen evolved rapidly on electrode B and that the lead-oxide layer formed on this electrode was less adherent than those produced on the other electrodes. Corrosion currents on all electrodes decreased significantly with

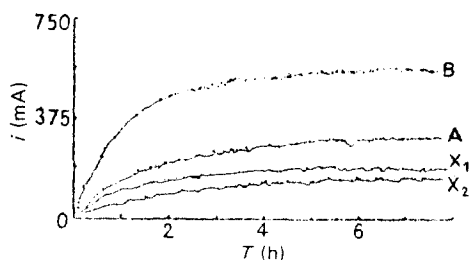


Fig. 2. Comparison of corrosion rates on four lead alloys.

decrease in either temperature or potential. When the temperature approaches  $50^{\circ}\text{C}$  and the potential is more positive than  $+1.40\text{ V}$ , the corrosion currents increased sharply, particularly for electrode B.

Each electrode I was polished, immersed in  $1\text{ M HNO}_3$  for several seconds, and then rinsed with distilled water, dried with filter paper, and placed in  $5.3\text{ M H}_2\text{SO}_4$ . The electrodes were polarized at a constant current of  $5\text{ mA}$  for  $15\text{ min}$ , and then cyclic voltammograms and polarization curves were measured. The electrodes were further corroded in the same solution at  $50^{\circ}\text{C}$  and  $+1.00\text{ V}$  for  $6\text{ h}$ , and the cyclic voltammograms and polarization curves again determined.

The first voltammogram of electrode  $X_1$  before and after corrosion is given in Fig. 3. These show that the oxidation peak at  $1.20\text{ V}$  and the reduction peak at  $0.94\text{ V}$  virtually disappear after corrosion. Similar behaviour is observed with electrode  $X_2$ . The two peaks still exist, however, if the corrosion potential is above  $1.20\text{ V}$ . The voltammogram for electrode  $X_1$  after 70 cycles is shown in Fig. 4. With cycling, a distinct anodic current peak appears at  $1.50\text{ V}$ ; this may be due to the oxidation of  $\text{Pb(II)}$  to  $\beta\text{-PbO}_2$ .

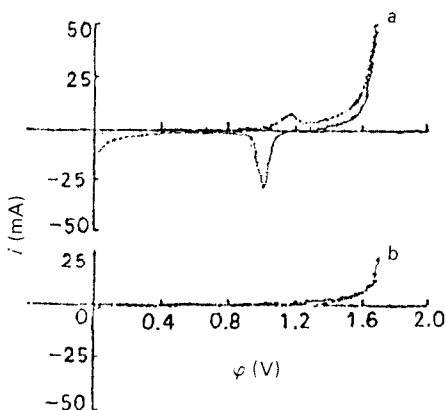


Fig. 3. Voltammograms for electrode  $X_1$ : (a) corrosion; (b) after corrosion. Scan rate  $60\text{ mV s}^{-1}$ .

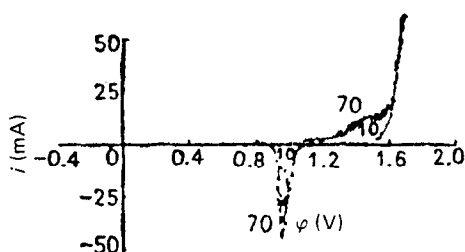


Fig. 4. Voltammogram for electrode  $X_1$  at cycle number 70. Scan rate  $60 \text{ mV s}^{-1}$ .

The peak is obscured by the current due to oxygen evolution. The voltammograms of the four different lead-alloy electrodes stabilized after 70 cycles.

The anodic polarization curves of electrode  $X_1$  before and after corrosion are given in Fig. 5. The curve before corrosion consists of three lines with different slopes, while after corrosion only 2 lines are present. Therefore, it is suggested that line 3 is the Tafel relationship for oxygen evolution, and lines 1 and 2 are associated with two oxidation steps of lead. The cathodic polarization curves of electrode  $X_1$  before and after corrosion are shown in Fig. 6. Prior to corrosion there are two reduction peaks: peak I at

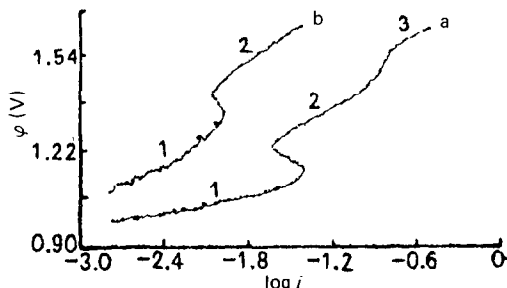


Fig. 5. Anodic polarization curves of electrode  $X_1$ : (a) before corrosion; (b) after corrosion at  $1.00 \text{ V}$ . Scan rate  $5 \text{ mV s}^{-1}$ .

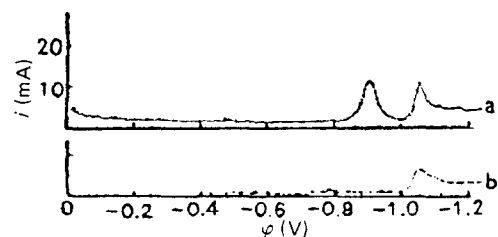


Fig. 6. Cathodic polarization curves of electrode  $X_1$ : (a) before corrosion; (b) after corrosion at  $1.00 \text{ V}$ . Scan rate  $5 \text{ mV s}^{-1}$ .

–0.95 V and peak II at –1.05 V. After corrosion, peak I disappears and peak II is shifted to a slightly more negative potential. By contrast, electrode B still exhibits the two peaks after corrosion. Furthermore, electrodes X<sub>1</sub> and X<sub>2</sub> display similar corrosion behaviour to that of electrode B if the corrosion potential is above 1.25 V and the temperature is 30 °C.

## Discussion

The corrosion-resistant ability of the positive grid is closely related to the composition, phase structure and intercrystalline contribution of the lead-oxide layer on the grid surface. In general, the anodic films formed in sulphuric acid solution consists of PbO and PbO<sub>2</sub> [3–5]. At low corrosion potentials, the lead-oxide layer contains PbSO<sub>4</sub>, PbO and  $\alpha$ -PbO. If the corrosion potential is above 0.90 V, the lead-oxide layer contains mainly  $\alpha$ -PbO<sub>2</sub> and  $\beta$ -PbO<sub>2</sub>. The  $\alpha$ -PbO<sub>2</sub> formed is compact, while  $\beta$ -PbO<sub>2</sub> is porous. The  $\beta$ -PbO<sub>2</sub> is formed only at the lead-oxide-layer/solution interface. The mechanism of corrosion of the lead electrode is related to the diffusion steps of O atom, O<sup>–</sup> ion, etc. Thus,  $\alpha$ -PbO<sub>2</sub> appears more corrosion-resistant than  $\beta$ -PbO<sub>2</sub>. PbO<sub>2</sub> on the lead surface catalyzes oxygen evolution [5]. The oxygen over-potential on  $\beta$ -PbO<sub>2</sub> is obviously higher than that on  $\alpha$ -PbO<sub>2</sub>.

The experimental results reported here show that lead is oxidized by oxygen atoms that are evolved from the PbO<sub>2</sub> thin layer and diffuse to the metal/oxide interface. The disappearance of the current peak shown in Fig. 3 may be due to the compactness of the oxidation layer which may be composed mainly of  $\alpha$ -PbO<sub>2</sub>. The intercept and the slope of the Tafel line (in Fig. 5) both increased after corrosion; the changes for electrodes X<sub>1</sub> and X<sub>2</sub> were more obvious than those for electrode B.

According to the composition of the lead-oxide layer formed after corrosion at 1.00 V for 6 h, the appearance of peak I and peak II (Fig. 6) suggests that PbO/PbSO<sub>4</sub> or PbSO<sub>4</sub> are reduced on the surface of the lead-oxide layer. Thus, it appears that PbO is absent in the lead-oxide layer of a Pb–Sr alloy, but with Pb–Sb alloys some Pb(II) oxide is observed. In other words, the lead-oxide layer formed on Pb–Sr alloys has a more perfect phase structure. This may be the main reason for the greater resistance of Pb–Sr alloys.

## References

- 1 U. B. Thomas, *Bell Lab. Rec.*, **16** (1973) 12.
- 2 J. Burbank, A. C. Simon and E. Willihnganz, in P. Delahay and C. M. Tobias (eds.), *Advances in Electrochemistry and Electrochemical Engineering*, Vol. 8. Wiley, New York, 1971, p. 157.
- 3 M. A. Dasoyang and I. A. Agoof, *Energy*, **10** (1981) 182.
- 4 Jiang Zhiyun, *Chinese Batteryman Q.*, **1** (1983) 5–8.
- 5 I. H. Razina, *Rep. Sci. Acad. U.S.S.R.*, **111** (1956) 404–406 (in Russian).